

Development of a New Design Methodology for Structural Airfield Mats

Carlos R. Gonzalez¹ and Timothy W. Rushing¹⁺

Abstract: The U.S. Army Engineer Research and Development Center (ERDC) is currently evaluating the performance of aluminum, fiberglass, plastic, and composite airfield mats under both F-15 and C-17 aircraft loads. Historically, the design methodology to determine the number of aircraft passes that a particular airfield mat will sustain before failure has been empirically correlated to the subgrade California Bearing Ratio (CBR) and the equivalent single-wheel load. A new mechanistic design approach was developed in which the performance of the airfield mat is related to the maximum deviator stress being applied to the subgrade. New design criteria relating this deviator stress to the number of passes for aircraft wheel loads were also developed. A new mat response model as well as comparisons to experimental measurements collected from full-scale traffic test sections conducted at the ERDC is presented in this paper to show the applicability of the new design procedure.

Key words: Airfield mat; AM2; Landing mat; Portable pavement; Temporary pavement.

Introduction

This paper summarizes an investigation conducted at the U.S. Army Engineer Research and Development Center (ERDC) to improve the design of airfield mats subjected to F-15 and C-17 aircraft landing gear loads. Airfield mats are portable pavement systems that connect using interlocking mechanisms, are installed over semi-prepared subgrades, and are designed to support aircraft wheel loads. The term coverage, as used in this paper, must be defined in terms of a single point on the pavement surface. A coverage occurs anytime an aircraft tire crosses this single point. The pass-to-coverage ratio is the inverse of the sum of probabilities that the aircraft tire will cross a given point on the pavement during a pass. For this study, the pass-to-coverage ratios were 4.0 and 1.12 for the F-15 and C-17 aircraft, respectively. These values were calculated based on normally distributed traffic patterns used in full-scale test sections at the ERDC. The experimental designs were based on theoretical lateral normal distributions of aircraft traffic and were verified by actual field measurements in earlier studies [1].

The previous design method, dating back to the 1950s, was completely empirical and was based on the original CBR design equation for flexible pavements below [2]:

$$t = (0.23 \log C + 0.15) \sqrt{\frac{P}{8.1 CBR} - \frac{A}{\pi}} \quad (1)$$

In Eq. 1, t is the total thickness of flexible pavement structure above the subgrade in inches, C is the number of aircraft coverages, P is the single or equivalent single-wheel load in pounds, CBR is the measure of subgrade strength, and A is the tire contact area in square inches. By using the CBR equation, a required thickness of flexible pavement structure was calculated that provided the same

load support capability for each loading and subgrade condition found in actual airfield mat tests. The required thickness of select fill material under the mat required to protect the subgrade was calculated by subtracting the equivalent thickness of the mat from the standard flexible pavement thickness calculated by the CBR equation. Multiple full-scale test sections were constructed at the U. S. Army Engineer Waterways Experiment Station (now the ERDC) during the 1950s and 1960s to develop equivalency curves for different airfield mats. These equivalency curves were developed for a limited number of designs constructed from aluminum and steel.

Due to the development of several new airfield matting systems constructed of various materials, a new mechanistic design approach was needed. Recent airfield mat testing at the ERDC provided the necessary data for developing this new design approach. The airfield mat design investigation was conducted as part of the Joint Rapid Airfield Construction (JRAC) program sponsored by the U.S. Army and the Rapid Parking Ramp Expansion (RPRE) program, sponsored by the U.S. Air Force (USAF) Air Combat Command. The primary airfield matting objective of the JRAC program was to evaluate the structural requirements for contingency airfields in terms of the number of passes-to-failure of commercial off-the-shelf mat systems [3]. The main objective of the RPRE program was to establish the load-carrying capacity of the existing AM2 aluminum mat and to develop a new lighter-weight airfield mat system as a replacement [4-7]. The AM2 results were used as a baseline for comparison with the performance of new mat prototypes as they were developed. Full-scale test sections were constructed at the ERDC and trafficked with C-17 and F-15 aircraft load simulators. Data were collected from these two projects and combined to establish airfield mat material properties, performance criteria under traffic, and design procedures for subgrade strength and thickness requirements underneath the mat systems. From the results of these traffic tests, new airfield mat criteria were developed based on the mechanistic stress-based criteria parameter (beta criteria) recently developed for the design of flexible pavements [8].

Airfield Mat Properties

¹ P.E., Airfield and Pavements Branch, Geotechnical and Structures Laboratory, U.S. Army Engineer Research and Development Center, Vicksburg, MS 39180-6199, USA.

⁺ Corresponding Author: E-mail Timothy.W.Rushing@usace.army.mil
 Note: Submitted September 25, 2009; Revised December 15, 2009;
 Accepted December 16, 2009.

Table 1. Back-Calculated Flexural Rigidity for the Mats Tested.

Mat	Material	Panel Size <i>cm x cm (ft. x ft.)</i>	Number Panels Tested	Direction Of Testing	Unit Thickness <i>cm (in.)</i>	Modulus Elasticity <i>MPa (ksi)</i>	Possion's Ratio	Flexural Rigidity <i>N-m (kips-in.)</i>
AM2 Test1	Aluminum	61 x 183 (2 x 6)	1	Long	3.8 (1.5)	27,372 (3,970)	0.2	131,401 (1,163)
AM2	Aluminum	61 x 183 (2 x 6)	3	Long	3.8 (1.5)	25,166 (3,650)	0.2	120,781 (1,069)
AM2	Aluminum	61 x 183 (2 x 6)	1	Long	3.8 (1.5)	22,201 (3,220)	0.2	106,545 (943)
AM2 Mod6	Aluminum	122 x 213 (4 x 7)	1	Long	3.8 (1.5)	11,790 (1,710)	0.2	56,605 (501)
AM2 Mod6	Aluminum	122 x 213 (4 x 7)	2	Long	3.8 (1.5)	22,270 (3,230)	0.2	106,884 (946)
AM2 Mod6	Aluminum	122 x 213 (4 x 7)	1	Short	3.8 (1.5)	2,344 (340)	0.2	11,298 (100)
M19	Aluminum	122 x 122 (4 x 4)	1	Long	3.8 (1.5)	3,447 (500)	0.2	16,496 (146)
M19	Aluminum	122 x 122 (4 x 4)	2	Long	3.8 (1.5)	1,531 (222)	0.2	7,344 (65)
Prototype 1	Aluminum	122 x 213 (4 x 7)	1	Long	3.8 (1.5)	9,308 (1,350)	0.2	44,742 (396)
Prototype 1	Aluminum	122 x 213 (4 x 7)	2	Long	3.8 (1.5)	9,584 (1,390)	0.2	45,985 (407)
Prototype 2	Aluminum	61 x 213 (2 x 7)	1	Long	3.8 (1.5)	24,201 (3,510)	0.2	116,148 (1,028)
Prototype 3	Composite	128 x 213 (4.2 x 7)	1	Long	5.1 (2.0)	6,826 (990)	0.2	77,734 (688)
Prototype 3	Composite	128 x 213 (4.2 x 7)	2	Long	5.1 (2.0)	3,758 (545)	0.2	42,708 (378)
Prototype 3	Composite	128 x 213 (4.2 x 7)	1	Short	5.1 (2.0)	1,517 (220)	0.2	17,287 (153)
ACE Mat	Fiberglass	204 x 204 (6.7 x 6.7)	1	Long	1.3 (0.5)	1,896 (275)	0.2	339 (3)
Bravo Mat	HDPE	122 x 122 (4 x 4)	1	Long	7.0 (2.75)	179 (26)	0.3	5,649 (50)
Bravo Mat	HDPE	122 x 122 (4 x 4)	2	Long	7.0 (2.75)	117 (17)	0.3	3,728 (33)
ACE-4Ply	Fiberglass	204 x 204 (6.7 x 6.7)	1	Long	0.32 (0.125)	303 (44)	0.5	1,017 (9)
ACE-4Ply	Fiberglass	204 x 204 (6.7 x 6.7)	2	Long	0.32 (0.125)	262 (38)	0.5	904 (8)
ACE-5Ply	Fiberglass	204 x 204 (6.7 x 6.7)	1	Long	0.40 (0.156)	186 (27)	0.5	1,243 (11)
ACE-5Ply	Fiberglass	204 x 204 (6.7 x 6.7)	2	Long	0.40 (0.156)	124 (18)	0.5	904 (8)
Dura Base	HDPE	244 x 427 (8 x 14)	1	Long	10.2 (4.0)	324 (47)	0.3	30,845 (273)
Dura Base	HDPE	244 x 427 (8 x 14)	2	Long	10.2 (4.0)	462 (67)	0.3	44,403 (393)
Dura Base	HDPE	244 x 427 (8 x 14)	1	Long	10.2 (4.0)	317 (46)	0.3	30506 (270)



Fig. 1. Test Setup to Back-calculate Mat Composite Flexural Rigidity.

Ten different airfield mats were evaluated at the ERDC test facility. These airfield mats were manufactured of different material types, thicknesses, and core structure designs. A list of these airfield mats and some of their physical properties are listed in Table 1. The structural properties of these airfield mats were determined from a simply-supported beam test setup [5]. Each airfield mat was placed across two supporting beams and loaded with lead and steel blocks of known weights. The deflection of the mat surface was measured

with deflection gauges placed underneath the airfield mat, as illustrated by Fig. 1. Mats were tested in single- and multiple-panel configurations to evaluate the influence of the panel joint system. Typical load-time responses for the AM2 and Durabase® airfield mats are shown in Figs. 2 and 3. The aluminum and carbon mats did not creep under load, but the polymeric mats exhibited viscoelastic properties. The viscoelastic mat behavior was addressed by allowing the load to remain in place until the deflection stabilized before additional load was applied. The flexural rigidity of the airfield mats was back-calculated from these deflection basins using finite element implementation of the Mindlin plate solution [9]. The actual test setup was modeled with the mats characterized as three dimensional plates with a fixed thickness. Loads were applied to the model to represent the conditions used for testing. The poisson ratio, ν , of each mat was fixed to values shown in Table 1, and the modulus of elasticity, E , of the mats was varied in the finite element model until a match between the predicted and measured deflections was achieved. Once the deflections matched, the plate flexural rigidity, D , was calculated using chosen values of E and ν in the equation $D = Eh^3/12(1-\nu^2)$. Fig. 4 shows typical results for the AM2 mat. From these curves, representative flexural rigidity (and corresponding modulus of elasticity and Poisson ratio) was chosen to model the cross section of the airfield mat. These values are displayed in the last column of Table 1.

Description of Test Sections

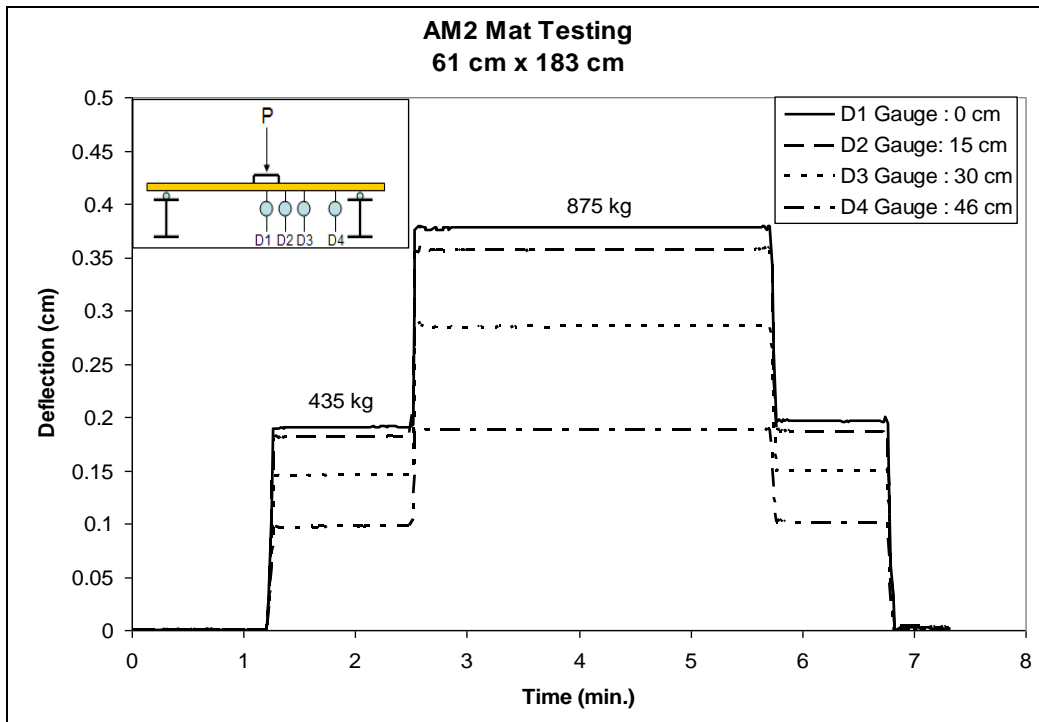


Fig. 2. Sample Loading Response for AM2 61-cm by 183-cm Airfield Mat.

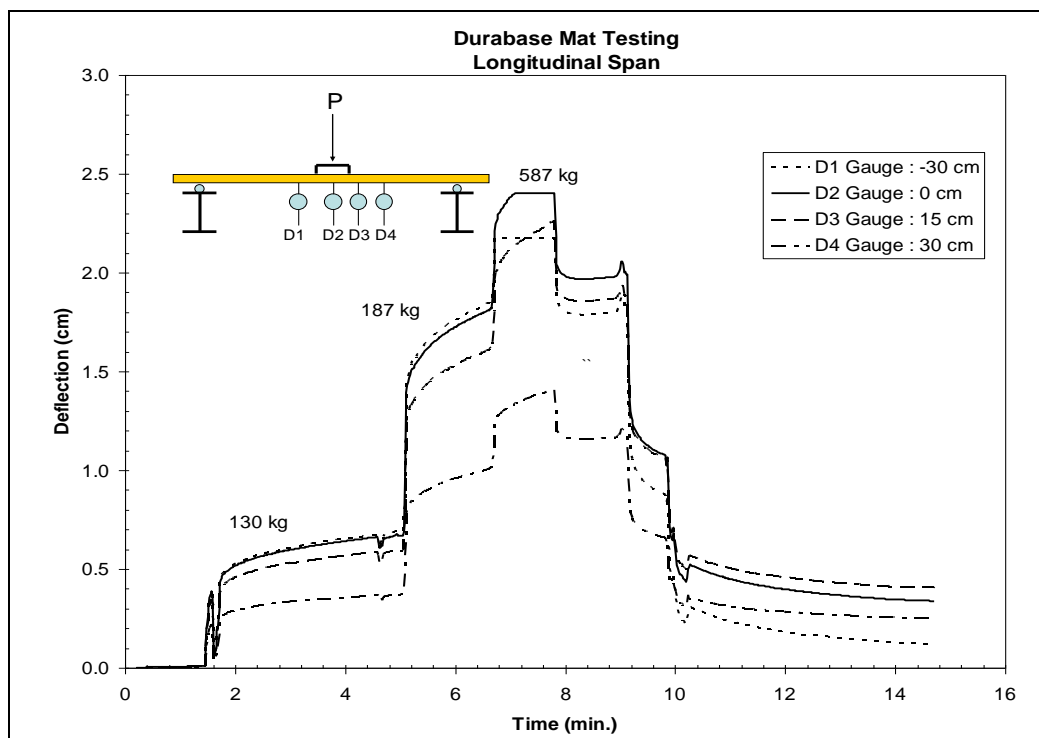


Fig. 3. Sample Loading Response for Durabase® 244-cm by 427-cm Airfield Mat.

Most of the data gathered for the development of the new airfield mat design procedure were collected from the RPRE project. Full-scale mat test sections were constructed and trafficked with simulated F-15 or C-17 load carts until failure [4-7]. The type of

traffic applied to each mat system is shown in Table 2. The F-15 load cart represented a 15,982-kg (35,235-lb.) single-wheel gear with a tire pressure of 2,241kPa (325psi) (Fig. 5). The C-17 load cart represented a six-wheel 122,270-kg (269,560-lb.) gear with tire

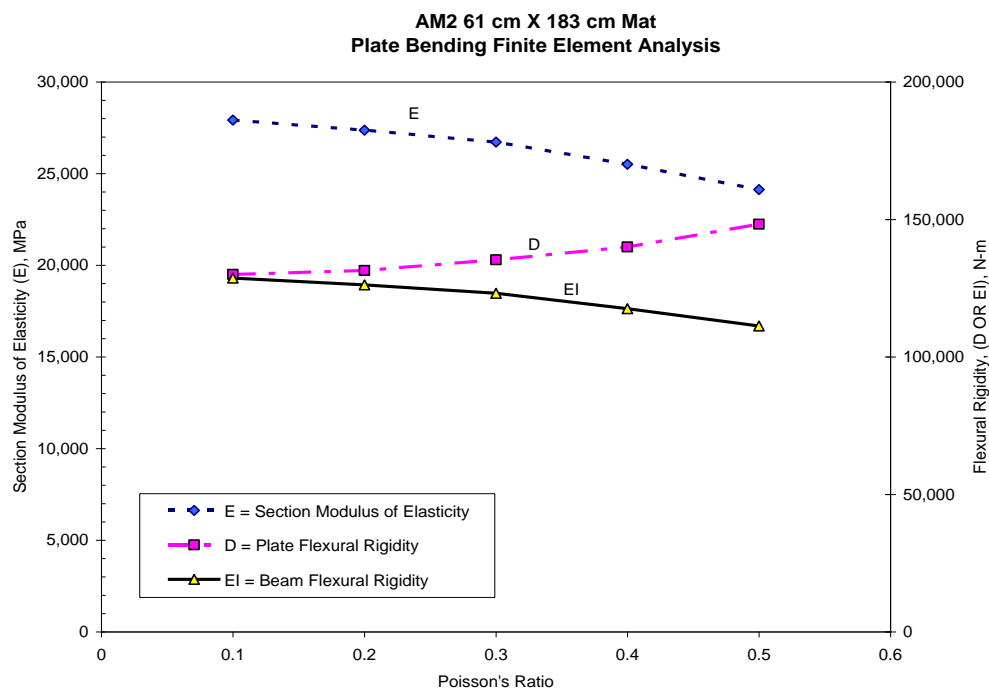


Fig. 4. Plate Bending Analysis of AM2 61-cm by 183-cm Airfield Mat.

Table 2. Airfield Mat Performance Data from Developed Criteria.

Test Section	Aircraft	Load <i>kg (lb.)</i>	Tire Pressure <i>kPa (psi)</i>	Airfield Mat Type	Coverages To Failure	Subgrade CBR	Deviator Stress <i>kPa (psi)</i>	Beta <i>kPa (psi)</i>
RPRE	F-15	15,982 (35,235)	2,241 (325)	AM2	384	6	391 (56.70)	205 (29.69)
RPRE	F-15	15,982 (35,235)	2,241 (325)	AM2	721	10	494 (71.60)	155 (22.49)
RPRE	F-15	15,982 (35,235)	2,241 (325)	AM2	1029	15	590 (85.60)	124 (17.93)
RPRE	F-15	15,982 (35,235)	2,241 (325)	AM2 Mod6	228	6	431 (62.50)	226 (32.72)
RPRE	F-15	15,982 (35,235)	2,241 (325)	M19	448	6	899 (130.23)	434 (62.94)
RPRE	F-15	15,982 (35,235)	2,241 (325)	Prototype 3	1033	6	504 (73.03)	264 (38.24)
RPRE	F-15	15,982 (35,235)	2,241(325)	Prototype 1	12	6	627 (91.00)	329 (47.65)
RPRE	F-15	15,982 (35,235)	2,241 (325)	Prototype 2	96	6	414 (60.10)	217 (31.47)
RPRE	C-17	20,380 (44,930)	979 (142)	AM2	1375	6	342 (49.60)	179 (25.97)
RPRE	C-17	20,380 (44,930)	979 (142)	AM2	5404	10	397 (57.56)	125 (18.08)
RPRE	C-17	20,380 (44,930)	979 (142)	AM2	6336	15	442 (64.10)	93 (13.42)
JRAC	C-17	20,380 (44,930)	979 (142)	ACE 5-Ply	275	9	614 (89.10)	214 (31.10)
JRAC	C-17	20,380 (44,930)	979 (142)	DuraBase	125	5.5	458 (66.40)	262 (37.93)

pressures of 979kPa (142psi) (Fig. 6). Each test section consisted of the designated mat system placed directly on top of a 91-cm deep (36-in.) high-plasticity clay subgrade constructed to produce a specific subgrade CBR. Test section CBR values ranged from 5.5 to 15 as shown in Table 2 for respective matting systems. Each mat system was placed on top of the prepared subgrade and trafficked until failure. The failure criteria for these mats were set to minimize tire damage, permanent surface deformation, subgrade rutting, and surface roughness. A test section was considered failed when a minimum 10% of the panels suffered structural damage (tears in excess of 15cm (6in.), bending in excess of 1.5cm (0.6in.), sharp edges or corners creating tire hazards, or mat instability under traffic). Failure also occurred if the mat section produced a

permanent surface deformation, subgrade rutting, or abrupt change in elevation of 3.2cm (1.25in.) for the F-15 or 7.6cm (3.0in.) for the C-17 gear. These matted test sections were instrumented with earth pressure cells to record the ability of the mats to distribute the applied vertical stresses to the subgrade. The measured vertical subgrade stresses were used to develop a correlation between applied coverages-to-failure and an indicator of performance known as the beta factor. This beta factor is described in the next section.

Description of an Airfield Mat Model

The airfield mat model was derived from the same physical model developed at the ERDC for the design of flexible pavements [8]. In



Fig. 5. F-15E Single-Wheel Load Cart with Guides for Traffic Lane Alignment.



Fig. 6. Multiple-Wheel C-17 Load Cart on the AM2 Test Section.

this model, the performance of conventional flexible pavements is quantified by the use of a beta factor defined as:

$$\beta = \frac{\sigma_f \cdot \pi}{CBR} \quad (2)$$

In this equation, σ_f is the vertical or deviator stress and CBR is the subgrade California Bearing Ratio. The σ_f represents the maximum stress transmitted to the subgrade through the pavement layers. In the case of conventional flexible pavements, this stress is transmitted through the shear resistance of the asphalt, base, and subbase layers composing the pavement structure. In the case of the airfield mat, this stress is transmitted due to the bending action or stiffness of the mat itself. The ability of the pavement structure (asphalt, base, subbase, or airfield mat) to distribute and reduce the applied load can be calculated by using Froolich's stress distribution equation [10, 11].

$$\sigma_z = \sum_{i=1}^{N_{lines}} \sum_{j=1}^{N_{loads}} \frac{n \cdot P_{i,j}}{2 \cdot \pi \cdot z^2} \cdot \cos^{n+2} \theta_{ij} \quad (3)$$

In this equation, σ_z is the calculated vertical stress at depth z , and n is the exponent that dictates the amount of load "dispersion" due to a point load P . The solution of a single concentrated point load is extended to a uniformly loaded area by subdividing the tire contact area into very small elemental rectangles, each in turn replaced by a concentrated load applied at its centroid. The

individual contribution of each elemental rectangular area is superimposed and summed to compute the total stress at some depth z . Similarly, the sum effect of multiple wheels is considered by following the procedure just described for a single wheel, creating a search grid within the gear, and calculating stresses at depth z until a maximum stress value is determined.

In general, the n exponent in Eq. (3) varies depending on the supporting subgrade CBR and the material from which the pavement is constructed. In the case of flexible pavements, n usually varies between 1 and 3 with a typical value of $n = 2$. A value of $n = 3$ represents a linear elastic, isotropic pavement response modeled by the Boussinesq or layered elastic stress solution. However, numerous analyses of matted sections performed in this project suggested that an n value equal to 3 may be used without introducing significant errors. Fig. 7 illustrates vertical stress data collected from studies conducted on unsurfaced pavements [12]. From Fig. 4, the predicted stresses using a value of $n = 3$ closely approximates the measured vertical stresses. The use of $n = 3$ in the airfield mat model greatly simplifies handling the predictions of stresses under mats since any layered elastic computer software can be used to compute predicted stresses under loads. To verify this concept, earth pressure cells were installed at depths of 30.5cm (12 in.) and 61cm (24in.) underneath an AM2 mat section trafficked with a simulated F-15 aircraft [6]. Measured vertical stresses were 372kPa (54psi) and 152kPa (22psi), respectively for 30.5cm (12in.) and 61cm (24in.) depths. Predicted vertical stresses using modulus values from Table 1 and layered elastic analyses were 386kPa (56 psi) and 159kPa (23psi), respectively. The process was repeated for the C-17 multi-wheel gear loading with similar results. Measured pressure values were 359kPa (52psi) and 193kPa (28psi) at depths of 30.5cm (12in.) and 61cm (24in.), while predicted values were 352 kPa (51psi), 186kPa (27psi). The closeness of the measured versus predicted values validates the use of layered elastic analyses in the model.

Theoretical Landing Studies (TM 3-418)

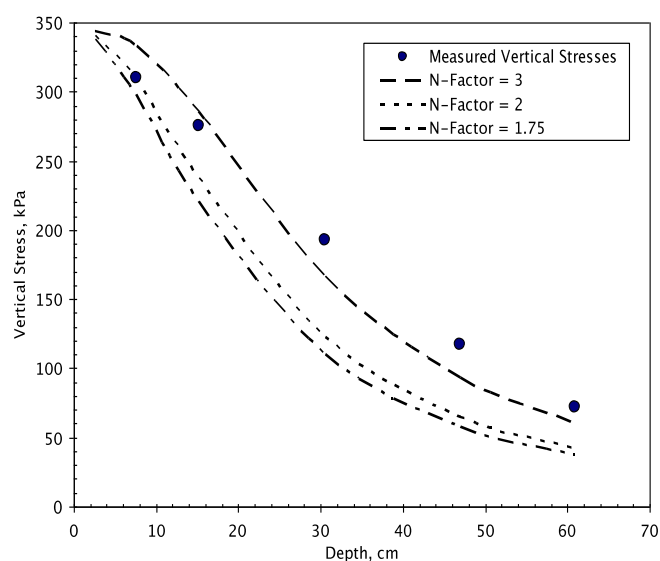


Fig. 7. Comparison between Measured and Predicted Vertical Stresses Using the Stress Distribution Factor Model Within an Unsurfaced Pavement.

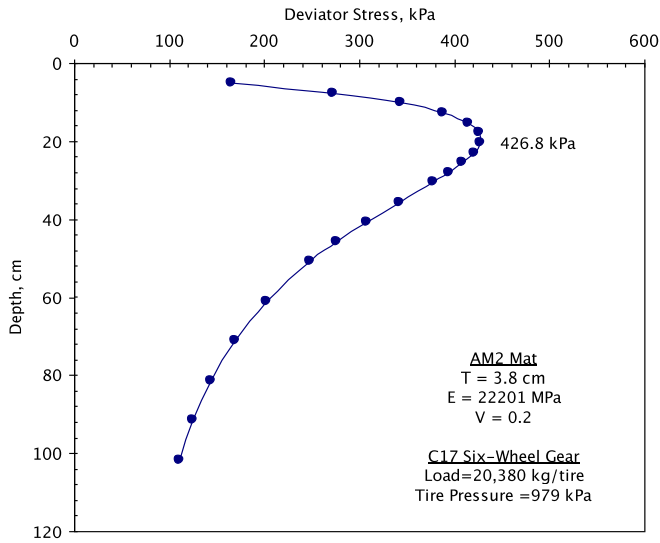


Fig. 8. Curve Showing the Relationship between Deviator Stress and Depth for a Six-Wheel C-17 Gear.

Using the data presented in Table 1 for each mat type (modulus of elasticity and poisson ratio), a system can be developed to compute the maximum vertical or deviator stress underneath a mat. This data can be used to develop an airfield mat performance model based on the beta criteria described by Eq. (2). The airfield mat panels and subgrade can now be treated and analyzed as a standard layered pavement system.

Airfield Mat Design Procedure Development

Performance data were generated for this study using the beta criteria described by Eq. (2), the ERDC windows based layered elastic analysis computer program (WINJULEA) [13], and the results of the mat testing provided in Table 1. These performance data are summarized in Table 2. An example plot showing the manner in which the deviator stress varies with depth is shown in

Fig. 8. The maximum deviator stress is then substituted into Eq. 2, along with the corresponding subgrade CBR, to calculate the beta value for a given test section. Knowing the beta value and the corresponding coverages-to-failure of a particular test item from full-scale traffic tests, a correlation between beta and coverages-to-failure was established. The number of coverages-to-failure and beta values computed for the various test sections were used to develop the performance criteria depicted in Fig. 9. Although this performance criterion is based on a limited number of tests, an excellent trend is shown as indicated by the R-squared of 0.73 for the series of full-scale tests performed, with the exception of one outlier, M19. The reason for this outlier is thought to be related to the geometry of the M19 panel. The normal distribution of traffic under the F-15E aircraft is 152-cm (5-ft.) wide. An M19 panel is only 122-cm (4-ft.) wide and, therefore, fits entirely inside the traffic lane. Additional longitudinal joints are incorporated in the traffic region and, therefore, allow the global system to become more flexible. Due to the complexity of the system and the nature of the narrow panel geometry, a rigid plate analysis may not be suitable for M19. A flexible pavement model may better characterize systems with narrow panel configurations. Since the trend in Fig. 9 fits for the other airfield mat designs constructed from various materials and M19 is no longer manufactured, the data were considered by the authors to be reasonable for implementation in a new mechanistic procedure. This procedure was used for the creation of design curves for airfield mat systems.

The implementation procedure for this new airfield mat criterion follows the same procedure introduced for the design of flexible pavements using the beta criteria [8]. From these beta criteria and the airfield mat properties contained in Table 1, design charts can be created such as the one shown in Fig. 10 for the C-17 aircraft operating on AM2 mats. Each curve in these charts is developed by calculating the thickness required under a specific mat, (using the layered elastic model and the performance criteria developed in this study) for a range of subgrade strengths (CBR), using a design pass

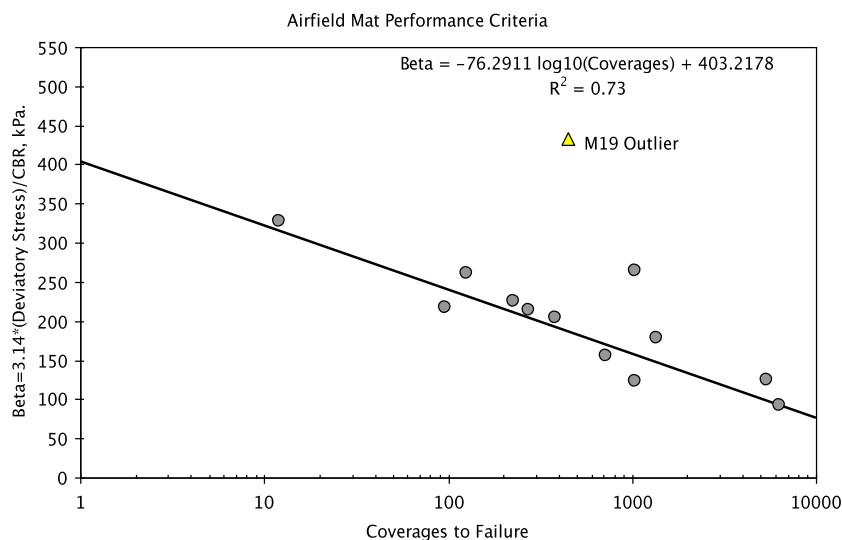


Fig. 9. Airfield Mat Performance Based on Beta Criteria (Using Deviator Stress Computed with a Layered Elastic Computer Program).

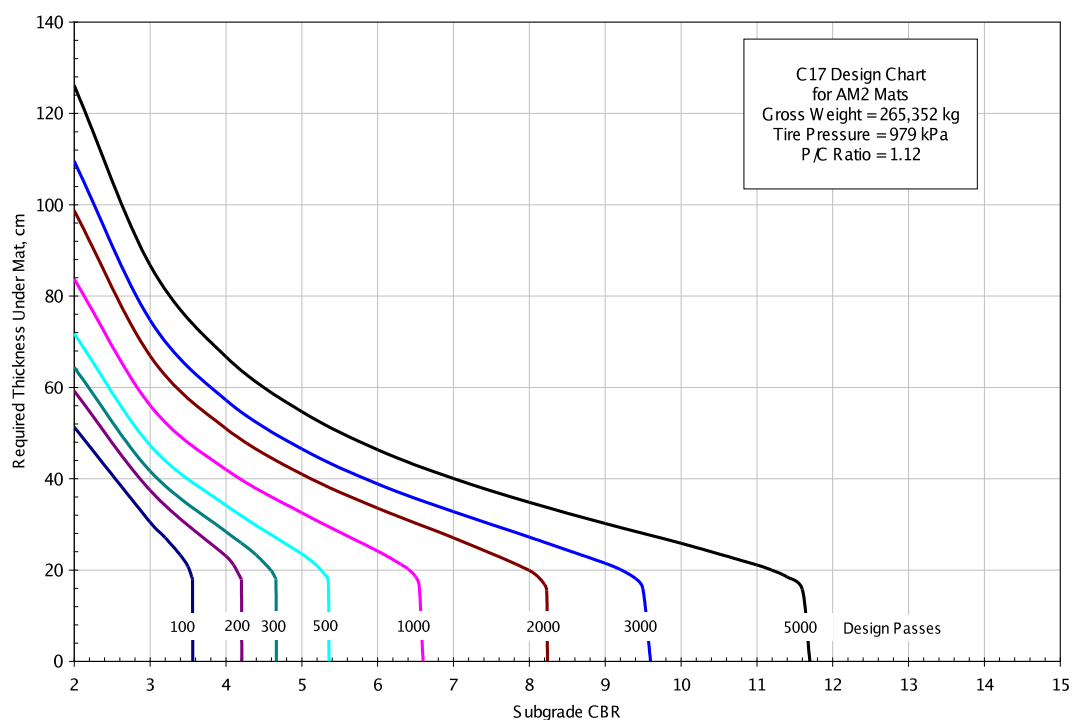


Fig. 10. AM2 Design Curve for the C-17 Aircraft Loaded at Gross Weight of 265,352kg (585,000lb.).

level for a given aircraft. This process is repeated for multiple design passes. From the design chart, the user can determine the amount of preparation required to the existing subgrade to achieve an operational requirement. For example, if the user needed to achieve 1,000 passes of a C-17 aircraft, a minimum of a 7 CBR subgrade would be required. If a soil investigation determined that the material 25cm (10in.) underneath the surface was a 4 CBR, 43 cm (17in.) of a 7 CBR or greater would be required to protect the 4 CBR material. Therefore, 18cm (7in.) of new material, 7 CBR or greater, must be added over the existing subgrade before mat placement in order to achieve the required pass level. Similar design charts can be generated for other types of airfield mats, aircraft, and aircraft weights.

Conclusions

The results of stiffness measurements, full-scale aircraft traffic testing, and layered elastic analyses support the implementation of a mechanistic stress-based design procedure for airfield mats to replace the existing completely empirical procedure developed in the 1950s. It can be concluded that the utilization of a stress-based criterion in terms of deviator stress versus coverages-to-failure closely predicts the actual performance of the tested airfield mats. The use of the layered elastic analysis procedure makes modeling the airfield mat simpler and enables the development of a more descriptive and mechanistic performance criteria.

Acknowledgement

The airfield mat experiments and resulting full-scale test data

presented in this paper were obtained from research conducted at the ERDC Geotechnical and Structures Laboratory, Airfield and Pavements Branch with funds provided by Headquarters, U.S. Army Corps of Engineers, Washington, DC and the U.S. Air Force through their offices at the Air Force Civil Engineer Support Agency, Tyndall, Florida. The support of the ERDC personnel is gratefully acknowledged, specifically Dr. Walter R. Barker, Terry Jobe, Tommy Carr, and Chad Gartrell.

References

1. Brown, D.N. and Thompson, O.O., (1973). Lateral Distribution of Aircraft Traffic, *Miscellaneous Paper S-73-56*, U.S. Army Corps of Engineers Waterways Experiment Station, Vicksburg, MS, USA.
2. Foster, C.R. and Burns, C.D., (1952). Development of Tentative CBR Design Curves for Landing Mats, *Miscellaneous Paper MP-4-29*, U.S. Army Corps of Engineers Waterways Experiment Station, Vicksburg, MS, USA.
3. Anderton G.L. and Gartrell, C.A., (2005). Rapid Maximum-On-Ground (MOG) Enhancement Technologies, *ERDC/GSL TR-05-2*, U.S. Army Engineer Research and Development Center, Vicksburg, MS, USA.
4. Rushing, T.W. and Tingle, J.S., (2006). AM2 and M19 Airfield Mat Evaluation for the RPRE Program, *ERDC/GSL TR-07-5*, U.S. Army Engineer Research and Development Center, Vicksburg, MS, USA.
5. Rushing, T.W. and Torres, N., (2007). Prototype Mat System Evaluation, *ERDC/GSL TR-07-29*, U.S. Army Engineer Research and Development Center, Vicksburg, MS, USA.

6. Rushing, T.W., Torres, N., and Mason, Q., (2008). AM2 10 CBR Subgrade Sensitivity Test for the Rapid Parking Ramp Expansion Program, *ERDC/GSL TR-08-13*, U.S. Army Engineer Research and Development Center, Vicksburg, MS, USA.
7. Rushing, T.W. and Mason, Q.S., (2008). AM2 15 CBR Subgrade Sensitivity Test for the Rapid Parking Ramp Expansion Program, *ERDC/GSL TR-08-25*, U.S. Army Engineer Research and Development Center, Vicksburg, MS, USA.
8. Barker, W.R. and Gonzalez, C.R., (2007). Renovation of the CBR Design Procedure, *Proceedings of the 2007 SWIFT Conference and Trade Show*, Calgary, Canada.
9. Mindlin, R.D., (1951). Influence of Rotatory Inertia and Shear on Flexural Motions of Isotropic Elastic Plates, *Journal of Applied Mechanics*, Vol. 18, pp. 31-38.
10. Jumikis, A.R., (1964). *Mechanics of Soils, Fundamentals for Advanced Study*, Chapters 3 and 4, D. Van Nostrand Company, Inc., Princeton, NJ, USA.
11. Jumikis, A.R., (1969). Stress Distribution Tables for Soil Under Concentrated Loads, *Engineering Research Publication No. 48*, College of Engineering, Rutgers University, NJ, USA.
12. U.S. Army Engineer Waterways Experiment Station, (1955). Theoretical Landing Mat Studies, *TM 3-418*, Vicksburg, MS, USA.
13. WINJULEA, (2003). Layered Elastic Analysis Software, Available Through the Pavement-Transportation Computer Assisted Structural Engineering (PCASE), Web Site www.pcase.com.